Available online at www.sciencedirect.com
ScienceDirect
Biochimica et Biophysica Acta 1758 (2006) 1621 – 1632
BIOCHIMICA ET BIOPHYSICA ACTA
BBA
www.elsevier.com/locate/bbamem

Production in *Escherichia coli* of a recombinant C-terminal truncated precursor of surfactant protein B (rproSP-$B_{\Delta c}$). Structure and interaction with lipid interfaces

Alicia G. Serrano, Elisa J. Cabré, José M. Oviedo, Antonio Cruz, Beatriz González, Alicia Palacios, Pilar Estrada, Jesús Pérez-Gil *

Dept. Bioquímica y Biología Molecular I, Facultad de Biología, Universidad Complutense, 28040 Madrid, Spain

Received 19 December 2005; received in revised form 28 July 2006; accepted 28 July 2006
Available online 3 August 2006

Abstract

SP-B, a protein absolutely required to maintain the lungs open after birth, is synthesized in the pneumocytes as a precursor containing C-terminal and N-terminal domains flanking the mature sequence. These flanking-domains are cleaved to produce mature SP-B, coupled with its assembly into pulmonary surfactant lipid–protein complexes. In the present work we have optimized over-expression in *Escherichia coli* and purification of rproSP-$B_{\Delta C}$, a recombinant form of human proSP-B lacking the C-terminal flanking peptide, which is still competent to restore SP-B function in vivo. rProSP-$B_{\Delta C}$ has been solubilized, purified and refolded from bacterial inclusion bodies in amounts of about 4 mg per L of culture. Electrophoretic mobility, immunoreactivity, N-terminal sequencing and peptide fingerprinting all confirmed that the purified protein had the expected mass and sequence. Once refolded, the protein was soluble in aqueous buffers. Circular dichroism and fluorescence emission spectra of bacterial rproSP-$B_{\Delta C}$ indicated that the protein is properly folded, showing around 32% α-helix and a mainly hydrophobic environment of its tryptophan residues. Presence of zwitterionic or anionic phospholipids vesicles caused changes in the fluorescence emission properties of rproSP-$B_{\Delta C}$ that were indicative of lipid–protein interaction. The association of this SP-B precursor with membranes suggests an intrinsic amphipathic character of the protein, which spontaneously adsorbs at air–liquid interfaces either in the absence or in the presence of phospholipids. The analysis of the structure and properties of recombinant proSP-$B_{\Delta C}$ in surfactant-relevant environments will open new perspectives on the investigation of the mechanisms of lipid and protein assembly in surfactant complexes.

Keywords: Lung surfactant; Protein folding; Inclusion body; Saposin-like protein; Lipid–protein interaction; Amphipathic protein

1. Introduction

Pulmonary surfactant is a complex mixture of lipids and proteins produced by type II pneumocytes. Surfactant is secreted into the very thin aqueous layer that covers the alveolar epithelium where it plays an essential role in reducing surface tension at the air–liquid interface to prevent alveolar collapse at the end of expiration.

There are four specific pulmonary surfactant proteins called SP-A, SP-B, SP-C and SP-D. The larger surfactant proteins, SP-A and SP-D, are hydrophilic, while SP-B and SP-C are small very hydrophobic polypeptides. Surfactant protein B is a homodimer, containing 79 amino acids per monomer, which plays a key role in pulmonary surfactant function. Reduction of alveolar SP-B content causes surfactant dysfunction and respiratory failure [1,2]. Mutations in the SP-B gene (SFTPB) that result in a complete absence of the mature protein in the airways are invariably fatal shortly after birth, demonstrating that SP-B is absolutely required for postnatal lung function and survival [1,3,4].

Human SP-B is synthesized by type II pneumocytes as a preproprotein of 381 amino acids. A signal peptide of 23

Abbreviations: CD, circular dichroism; DPPC, 1,2-dipalmitoyl-*sn*-glycero-3-phosphocholine; IPTG, Isopropyl-β-D-thiogalactopyranoside; MLV, Multilamellar vesicles; PBS, phosphate buffer saline; PMSF, phenylmethanesulphonyl fluoride; POPC, 1-palmitoyl-2-oleoyl-*sn*-glycero-3-phosphocholine; POPG, 1-palmitoyl-2-oleoyl-*sn*-glycero-3-phospho-*rac*-glycerol; SUV, Small unilamellar vesicles; SAPLIP, Saposin-like protein; TB, Terrific Broth culture medium; TEV, Tobacco etch virus

* Corresponding author. Tel.: +34 91 3944994; fax: +34 91 3944672.
E-mail address: jpg@bbm1.ucm.es (J. Pérez-Gil).

0005-2736/$ - see front matter © 2006 Elsevier B.V. All rights reserved.
doi:10.1016/j.bbamem.2006.07.016

residues (1–23) allows translocation of the precursor protein into the endoplasmic reticulum (ER). Along the exocytic pathway of type II cells proSP-B (24–381) is proteolytically cleaved in at least three different steps [5,6]. Cleavage of the N-terminal (24–200) and C-terminal (280–381) flanking domains generates the biophysically active mature SP-B. This hydrophobic peptide is positively charged and has been shown to promote aggregation, fusion and disruption of liposomes containing negatively charged phospholipids [7–10]. All these features make mature SP-B difficult to express as a recombinant protein in heterologous systems. Lin and coworkers [11] demonstrated that the N-terminal propeptide, consisting of the mature peptide and the N-terminal flanking domain, is necessary and sufficient for sorting and secretion of SP-B in different mammalian cell lines [12]. Expression of the N-terminal propeptide in SP-B knock-out mice completely restored lung function and normal surfactant composition, indicating that the C-terminal flanking domain is not required for SP-B processing and survival [13]. Considering the intrinsic hydrophobicity of mature SP-B and its propensity to interact with lipids, the intracellular transport of this molecule likely requires association with a hydrophilic chaperone-like element. In fact, Lin et al. [11] previously proposed that the N-terminal domain might fulfill this role, protecting SP-B from the environment until the precise time and location where lipids and proteins assemble.

ProSP-B is a transient intermediate in SP-B synthesis and does not accumulate in type II pneumocytes. Isolation and purification of this protein from natural sources in amounts sufficient for its characterization is therefore not feasible. The goal of the present work was to purify enough recombinant human proSP-B (rproSP-$B_{\Delta C}$) from a prokaryote expression system (*E. coli*) to initiate a detailed characterization of its structure and lipid-interacting properties.

2. Materials and methods

2.1. Expression, purification and refolding of rproSP-$B_{\Delta C}$

The cDNA sequence coding for proSP-$B_{\Delta C}$ (amino acids 24–381; GenBank® accession No. M24461, including mutations described in Fig. 1) was cloned into the *Eco*RI–*Xba*I sites of the bacterial expression vector pProEx-1 [14] (Life Technologies, Gaithersburg, MD, USA) (construct provided by Dr. T.E. Weaver, Cincinnati Children's Hospital Medical Center, Cincinnati, OH, USA). The sequence of the insert was confirmed by DNA sequencing and *Escherichia coli* UT5600 was transformed with this plasmid for expression.

Fig. 2 presents a scheme outlining the main steps of the strategy optimized to produce recombinant soluble proSP-$B_{\Delta C}$ in bacterial cultures. A single colony of *E. coli* UT5600 transformed with pProEx-1/proSP-$B_{\Delta C}$ plasmid (Fig. 3) was first grown overnight at 37 °C in 20 mL of LB medium containing 100 μg/mL ampicillin. The culture was then inoculated into 1 L of TB medium containing 100 μg/mL ampicillin and was grown to an $OD_{600\ nm}$ of 0.6–0.8. Induction was then performed by addition of IPTG to a final concentration of 0.25 mM. The culture was grown overnight at 37 °C and harvested by centrifugation at 5500×*g* for 20 min at 4 °C. The bacterial pellet was suspended in a volume of buffer A (50 mM sodium phosphate buffer, pH 7, containing 300 mM NaCl) equal to ten times its weight, and frozen until required. Cells were disrupted by incubation of the bacterial suspension for 20 min in the presence of 1 mg/mL lysozyme, 0.1 mM PMSF and 10 mM β-mercaptoethanol at room temperature, followed by tip sonication (2×2 min) in a digital sonifier II W-250 (Branson Ultrasonics, Danbury, CT, USA). After centrifugation for 20 min at 12,000×*g* and 4 °C, the pellet of inclusion bodies was resuspended for solubilization in a volume equal to 10 times its weight of buffer B (50 mM sodium phosphate, pH 7, 300 mM NaCl, 10 mM β-mercaptoethanol, 8 M urea) and sonicated (2×2 min). After overnight shaking at 4 °C the suspension was sonicated again and clarified by centrifugation for 20 min at 15000×*g*. The supernatant was applied to a 2 mL (bed volume) TALON™ metal affinity column (Clontech, Palo Alto, CA, USA). Chromatography was performed under denaturing conditions, as described by the supplier. Briefly, the column was washed twice with buffer B, the second time in the presence of 5 mM imidazole. rProSP-$B_{\Delta C}$ was eluted with buffer B containing 200 mM imidazole. Denaturing reagents and the other chemicals were eliminated from the eluates by successive dialysis at 4 °C to promote proper folding of the protein. Sequential dialysis was performed with the following buffers: buffer C, 50 mM sodium phosphate, pH 7, 150 mM NaCl, 10 mM β-mercaptoethanol, 5 M urea; buffer D, 50 mM sodium phosphate, pH 7, 150 mM NaCl, 10 mM β-mercaptoethanol, 1 M urea; buffer E, 50 mM sodium phosphate, pH 7, 300 mM NaCl; buffer F, 5 mM Tris, 150 mM NaCl, pH 7. Following dialysis, the protein solution was aliquoted and stored at −80 °C.

2.2. Electrophoresis and Western blot analysis

Sodium dodecylsulfate-polyacrylamide gel electrophoresis was performed using 12% and 4% acrylamide in the separating and stacking gels, respectively. Unless otherwise indicated, electrophoresis was performed under reducing conditions in the presence of 5% β-mercaptoethanol. Gels were stained with Coomassie brilliant blue R-250 (Applichem, Darmstadt, Germany). Alternatively, proteins were transferred to nitrocellulose membranes using a semidry transfer cell (Bio-Rad Laboratories, Hercules, CA, USA) set at 15 V for 25 min. Nitrocellulose membranes were blocked overnight at 4 °C in PBS containing

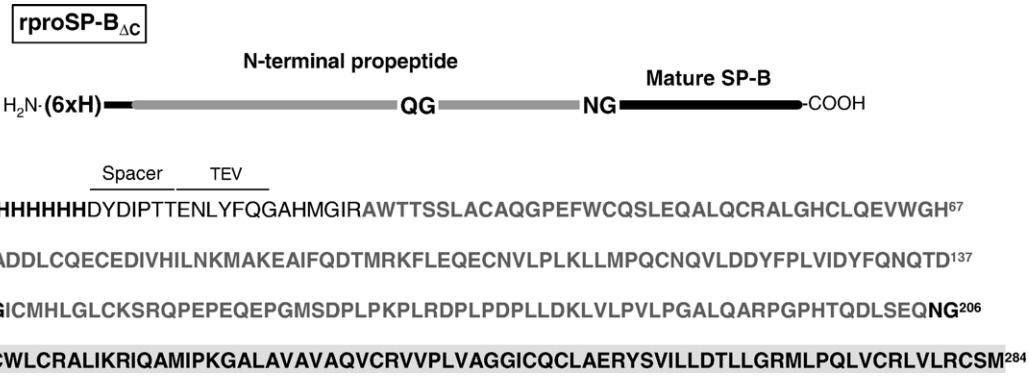

Fig. 1. Sequence of rproSP-$B_{\Delta c}$ protein. The N-terminal sequence of the recombinant protein includes a His_6-tag and a spacer region followed by the Tobacco etch virus (TEV) protease cleavage site to eventually remove the His-tag. A hydroxylamine cleavage site (NG) is present at the beginning of the SP-B mature sequence by the double substitution Q205N/F206G. An endogenous hydroxylamine cleavage site was eliminated by the additional amino acid substitution N139Q.

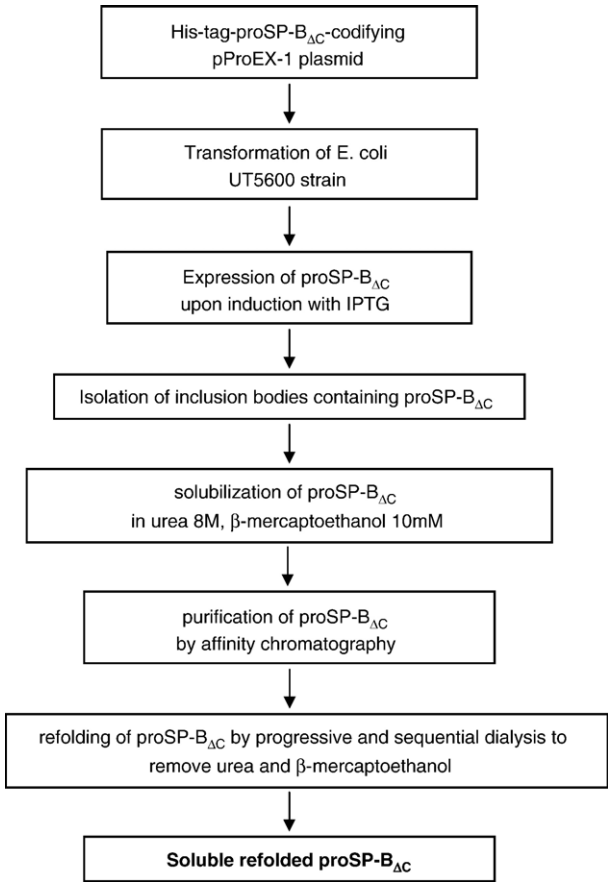

Fig. 2. Flow chart diagram of the procedure optimized to express, purify and refold rproSP-B$_{\Delta C}$ from bacterial cell cultures.

0.1% Tween-20 and 3% non-fat dried milk. Incubation with primary antibody was done using PBS containing 0.05% Tween-20 and 1.5% non-fat dried milk, for 2 h, at room temperature. Following washing with PBS containing 0.1% Tween-20, the membranes were incubated for another 2 h with the secondary antibody (peroxidase-conjugated) and washed again. The immunoblot was developed using luminol (Sigma, St. Louis, MO, USA) as a substrate for the chemiluminescent reaction. The primary antibodies used were an anti-His-tag peroxidase-conjugated monoclonal antibody (Sigma) or an anti-proSP-B monoclonal antibody, generously provided by Dr. T. E. Weaver (Cincinnati Children's Hospital Medical Center, Cincinnati, OH, USA). In the latter case, the secondary antibody was anti-mouse IgG peroxidase-conjugated (Sigma).

2.3. Protein analysis

Amino acid analysis of hydrolyzed rproSP-B$_{\Delta C}$ aliquots was performed on a Beckman 6300 automatic analyzer to accurately determine the protein concentration.

The NH_2-terminal sequence of rproSP-B$_{\Delta C}$ was determined by automated Edman degradation. After SDS-PAGE the protein was transferred to a polyvinylidene difluoride membrane (PVDF, BioRad, Richmond, CA, USA). Protein bands were identified by Coomassie blue staining, excised and microsequenced using a Procise 494 sequencer from Applied Biosystems.

2.4. Mass spectrometry analysis of protein spots

The gel spots of interest were manually excised from micro preparative gels using biopsy punches. Proteins selected for analysis were reduced in-gel, alkylated and digested with trypsin according to Sechi and Chait [15]. Briefly, spots were washed twice with water, shrunk 15 min with 100% acetonitrile and dried in a Savant SpeedVac for 30 min. Then the samples were reduced with 10 mM dithiotreitol in 25 mM ammonium bicarbonate for 30 min at 56 °C and subsequently alkylated with 55 mM iodoacetamide in 25 mM ammonium bicarbonate for 20 min in the dark. Finally, samples were digested with 12.5 ng/μl sequencing grade trypsin (Roche Molecular Biochemicals, Mannheim, Germany) in 25 mM ammonium bicarbonate (pH 8.5) overnight at 37 °C. After digestion, the supernatant was collected and 1 μl was spotted onto a MALDI target plate and allowed to air-dry at room temperature. Then, 0.4 μl of a 3 mg/ml of α-cyano-4-hydroxy-transcinnamic acid matrix (Sigma) in 50% acetonitrile was added to the dried peptide digest spots and allowed again to air-dry at room temperature. MALDI-TOF MS analyses were performed in a Voyager-DE-^{TM} STR instrument (PerSeptives Biosystems) fitted with a 337 nm nitrogen laser and operated in reflector mode with an accelerating voltage of 20000 V. All mass spectra were calibrated externally using a standard peptide mixture (Sigma). Peptides from the auto digestion of trypsin were used for the internal calibration. The analysis by MALDI-TOF mass spectrometry produces peptide mass fingerprints and the peptides observed can be collated and represented as a list of monoisotopic molecular weights. Data were collected in the *m*/*z* range of 700–2500. MS/MS sequencing analyses were carried out using the MALDI-tandem time-of flight mass spectrometer 4700 Proteomics Analyzer (Applied Biosystems, Framingham, MA).

2.5. Quantitation of free –SH groups

The presence of sulfhydryl (SH) groups in rproSP-B$_{\Delta C}$ was analyzed by using Ellman's reagent, 5,5′-dithiobis(2-nitrobenzoic acid) (DTNB) [16,17], in the absence or in the presence of 5 M guanidinium chloride. Ten-μg aliquots of rproSP-B$_{\Delta C}$ were incubated for 30 min at room temperature in 5 mM Tris buffer pH 8, containing 150 mM NaCl with or without 5 M guanidinium chloride. DTNB was then added to a concentration of 12.2 μM or 8.2 μM (final volume

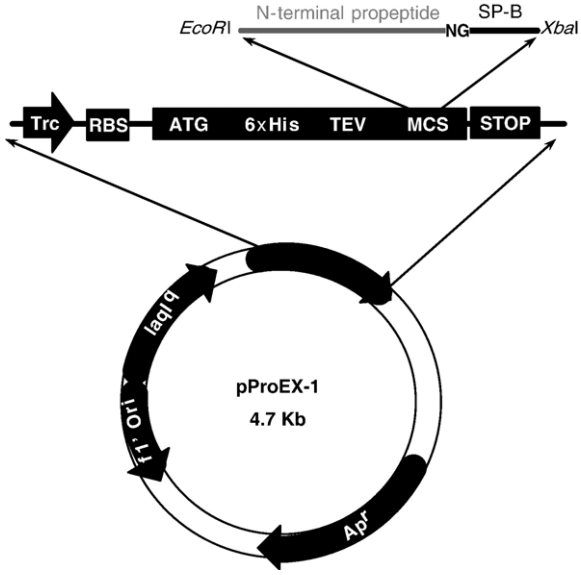

Fig. 3. Structure of pProEx-1/proSP-B$_{\Delta C}$, the expression plasmid of rproSP-B$_{\Delta C}$. The construct encoding a processing intermediate of human pulmonary surfactant protein B (GenBank® Accession No. M24461) proprotein, including the N-terminal propeptide and the mature protein (amino acids 24–279), is cloned between the *Eco*RI–*Xba*I restriction sites of pProEx-1 vector (Life Technologies, Gaithersburg, MD, USA). pProEx-1 vector includes a reiterative cytosine, adenosine, thymidine sequence at the 5′ end of the multicloning cleavage site (MCS) resulting in the incorporation of 6 His at the NH2-terminus of the recombinant protein. The vector also contains the cleavage site for TEV protease to eventually remove the His-tag from the fusion protein. The tryptophan lactose hybrid promoter Trc promoter and the l*ac*Iq gene preceding the ribosome binding site (RBS) allow high level of expression of the recombinant protein and tight regulation using IPTG.

1 mL), respectively, and $A^{412\ nm}$ was measured. After 10 min, absorbance measurements were interpolated in a calibration curve previously prepared from data of samples with different concentrations of free Cys in the same conditions described above.

2.6. Circular dichroism

Far-UV circular dichroism (CD) spectra were obtained in a Jasco-715 spectropolarimeter equipped with a xenon lamp [18]. The protein concentration was 0.1 mg/mL and the optical path length 0.1 cm. The CD spectra of the protein in membrane environments was obtained in the presence of unilamellar vesicles of 1-palmitoyl-2-oleoyl-*sn*-glycero-3-phosphocholine (POPC) or 1-palmitoyl-2-oleoyl-*sn*-glycero-3-phospho-*rac*-glycerol (POPG), selected as representative of zwitterionic and anionic membranes, respectively, and because these species are easily dispersed at 25 °C. The contribution of the buffer, as well as that of the phospholipid vesicles, when present, was always subtracted. A minimum of four spectra were accumulated for each sample. Values of mean residue ellipticity were calculated on the basis of 110 as the mean molecular weight per residue and are reported in terms of $[\theta]$ (degrees × cm^2 × $dmol^{-1}$). The secondary structure of the protein was evaluated by computer fit of the dichroism spectrum into four simple components (α-helix, β-sheet, turns and random coil) using the CDPro software package containing three commonly used programs: SELCON3, CONTIN/LL and CDSSTR [19,20]. This software allows the use of different sets of proteins to increase the reliability of analyses of membrane-interacting proteins, which is probably the case for highly lipophilic SP-B polypeptide.

2.7. Fluorescence emission spectroscopy

Tryptophan fluorescence emission spectra of rproSP-$B_{\Delta C}$ were recorded in a SLM-Aminco AB-2 spectrofluorimeter. The contribution of the buffer, as well as that of the phospholipid vesicles, when present, was always subtracted. Excitation wavelength was set at 275 nm or 295 nm and emission spectra were measured over the range of 300–440 nm. Both the excitation and emission slits were set at 4 nm. The contribution of tyrosine to the emission spectra was calculated, as previously described elsewhere [21], by subtracting the emission spectra measured at λ_{exc}=295 (multiplied by a normalizing factor) from the emission spectra measured at λ_{exc}=275 nm. This factor is the ratio between the fluorescence intensities measured with λ_{exc}=275 nm and λ_{exc}=295 nm at the emission wavelength of 380 nm, where no Tyr contribution is expected.

2.8. Preparation of phospholipid vesicles

Vesicles made of 1,2-dipalmitoyl-*sn*-glycero-3-phosphocholine (DPPC), POPC or POPG were prepared by hydrating dry lipid films in a 5 mM Tris, 5 mM Mes and 5 mM sodium acetate buffer, pH 7, containing 150 mM NaCl, and allowing them to swell for 1 h at room temperature (for POPC and POPG) or at 50 °C (for DPPC) with continuous shaking. This treatment typically produces multilamellar phospholipid suspensions (MLV). To obtain small unilamellar vesicles (SUV), the lipid suspensions were sonicated on ice (for POPC and POPG) or in a water bath at room temperature (for DPPC) using a Branson UP200s tip sonifier set at 360 w/cm^2, making cycles of 0.5 s for 2 min.

Samples containing phospholipid vesicles and rproSP-$B_{\Delta C}$ (used to analyze the effects of lipids in the circular dichroism or fluorescence spectra of the protein) were prepared by injection of the appropriate amount of protein into the phospholipid vesicle suspension followed by 10 min incubation at 37 °C.

2.9. Interfacial adsorption of rproSP-$B_{\Delta C}$

Adsorption of rproSP-$B_{\Delta C}$ to an open air–liquid interface was assayed using a specially designed surface balance as previously described [22]. The microbalance was filled with 1.5 mL of buffer (Tris 5 mM, NaCl 150 mM, pH 7) and, after 5 min equilibration, 30 μL of buffer containing 11 μg of protein were injected into the subphase. Changes in surface pressure (π) were then monitored over time. The subphase was continuously stirred and the trough was thermostated at 25 °C. Subphases were always prepared with double distilled water (the second distillation performed in the presence of potassium permanganate). Injection of equivalent volumes of buffer did not produce any detectable change in surface pressure.

2.10. Interaction of rproSP-$B_{\Delta C}$ with preformed phospholipids monolayers

Association of rproSP-$B_{\Delta C}$ with phospholipid monolayers, preformed at different initial surface pressures (π_i), was followed (in the same microbalance mentioned above) by monitoring changes in surface pressure ($\Delta\pi$) over time once the protein had been injected into the subphase (Tris 5 mM, NaCl 150 mM, pH 7, in double distilled water). Phospholipid monolayers were formed by spreading a concentrated solution of the lipids (typically DPPC:POPG, 7:3, w/w) in chloroform:methanol (3:1, v/v) on top of the aqueous surface. After 10 min equilibration, 11 μg of protein were injected into the subphase. The highest increment in surface pressure ($\Delta\pi$) after protein injection was plotted vs. the initial pressure (π_i) of the monolayer, allowing calculation of the critical insertion pressure (π_c), defined as the maximum π at which the protein can still insert. The subphase was continuously stirred and the temperature was kept constant at 25 °C during the experiment.

3. Results

3.1. Expression, purification and refolding of pro-SP-$B_{\Delta C}$

Expression of recombinant proSP-$B_{\Delta C}$ containing an N-terminal His_6-tag was carried out in TB media and induced by the addition of IPTG as described under Materials and methods. The sequence of the recombinant protein expressed is depicted in Fig. 1. In order to eventually separate mature SP-B from the N-terminal propeptide in future studies, a hydroxylamine cleavage site ($N^{205}G^{206}$) was inserted at the beginning of the mature sequence in place of the original QF pair in the sequence of wild type proSP-B. Chemical cleavage at this site should in principle produce a SP-B-like polypeptide with exactly the same length than native SP-B but having glycine instead of wild-type phenylalanine at the N-terminal end. The effect of this substitution for the surface activity of recombinant SP-B forms has to be established. A further additional single amino acid substitution eliminated an endogenous hydroxylamine cleavage site (N139Q). Fig. 4 clearly shows the time-dependent appearance of a protein band with an apparent molecular mass corresponding to that of the proSP-$B_{\Delta C}$ (31.8 kDa), and a minor band with apparent higher mobility, following IPTG induction. The recombinant protein accumulated in bacterial cells leading to the formation of inclusion bodies. Fig. 5 (a and b) shows the

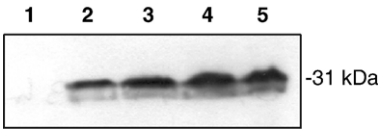

Fig. 4. Western blot analysis of rproSP-$B_{\Delta C}$ protein expressed after induction with IPTG. *E. coli* cells transformed with pProEx-1/proSP-$B_{\Delta C}$ before (lane 1) and after 0.5, 1, 2 or 3 h (lanes 2–5, respectively) induction with IPTG. Western blot was performed using mouse anti-His tag monoclonal antibodies (peroxidase-conjugated). The electrophoretic mobility of the detected major band was consistent with the expected molecular mass of rproSP-$B_{\Delta C}$ (31–32 kDa).

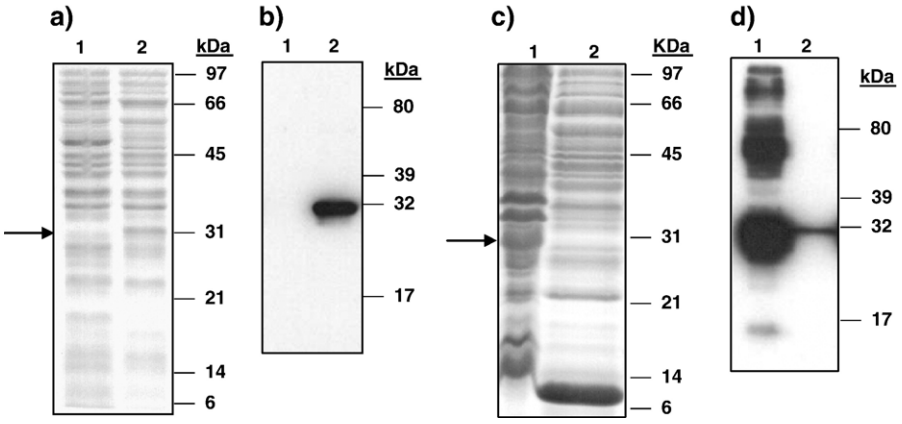

Fig. 5. Expression of rproSP-$B_{\Delta C}$ in *E. coli*. (a) SDS-PAGE analysis of UT5600 cells transformed with pProEx-1/proSP-$B_{\Delta C}$ before (lane 1) and after (lane 2) O/N induction. The electrophoresis was run under reducing conditions and the gels were stained with Coomassie blue. (b) Western blot analysis using an anti-proSP-B antibody of the same samples loaded in the Coomassie stained gel in panel a. (c) Coomassie blue stain SDS-PAGE analysis of rproSP-$B_{\Delta C}$ produced after O/N induction of bacteria. Cultures were harvested and centrifuged to eliminate the media. Cells were then resuspended in sodium phosphate buffer pH 7, containing NaCl 300 mM. After incubation in the presence of lysozyme and sonication, cells lysate were centrifuged to separate the pellet of inclusion bodies (lane 1) from the supernatant (lane 2). (d) Western blot analysis using an anti-proSP-B antibody of the same samples loaded in the Coomassie stained gel in panel c. Arrows indicate the position of rproSP-$B_{\Delta C}$, which has an expected molecular mass of ~31.8 kDa.

SDS-PAGE and Western blot analysis of pProEx-1/proSP-$B_{\Delta C}$ transformed UT5600 cells before and after O/N induction. A single band of recombinant protein, with an electrophoretic mobility corresponding to the expected molecular mass of a monomer of rproSP-$B_{\Delta C}$, was detected by Western Blot analysis. The same band can be distinguished in the Coomassie blue stained gel. No rproSP-$B_{\Delta C}$ band was detected prior to IPTG induction.

Isolation of inclusion bodies from bacteria pellets was performed as described under Materials and methods. After cell lysis using tip sonication and subsequent centrifugation, aliquots of the supernatant and the resuspended pellet were analyzed by 12% acrylamide gel electrophoresis. Most of the protein remained in the pellet of inclusion bodies after centrifugation as can be observed in Fig. 5 (c and d). A certain fraction of the protein was now observed to form dimers and oligomers of higher molecular mass, even though the main fraction migrated as a monomer. rProSP-$B_{\Delta C}$ was then purified by solubilization of inclusion bodies in 8 M urea followed by a metal affinity chromatography under denaturing conditions. The purified protein fractions were extensively dialyzed under progressively less denaturing conditions, as outlined in Materials and methods, to remove excess imidazole and to refold the protein. No visible precipitate was observed during dialysis, indicating that rproSP-$B_{\Delta C}$ is soluble at micromolar concentrations under these conditions. The purified and refolded protein was analyzed by 12% acrylamide gel electrophoresis followed either by Coomassie blue staining or Western blot analysis (Fig. 6). SDS-PAGE of purified rproSP-$B_{\Delta C}$ detected a single band after Coomassie blue staining, corresponding to the electrophoretic mobility of proSP-$B_{\Delta C}$ monomer. This mobility is slightly higher than that of most of the protein in the intact cells (see Fig. 4), probably as a consequence of the formation of some intramolecular disulphides (see below), once the protein is exposed to a partially oxidant environment, outside the cells. Western blot analysis also detected three minor bands with higher electrophoretic mobility than that of the putative recombinant protein band. All bands were detected using an anti-proSP-B monoclonal antibody as well as an anti-polyhistidine monoclonal antibody (not shown) suggesting that the three minor bands resulted either from partial degradation or incomplete translation of the recombinant protein. Mass spectrometry analysis of all protein spots from gel electrophoresis (not shown) confirmed this hypothesis. Densitometric analysis from Coomassie blue stained gels estimated that approximately 70–75% of the purified protein consisted of the species with apparent molecular mass of 31 kDa. Any

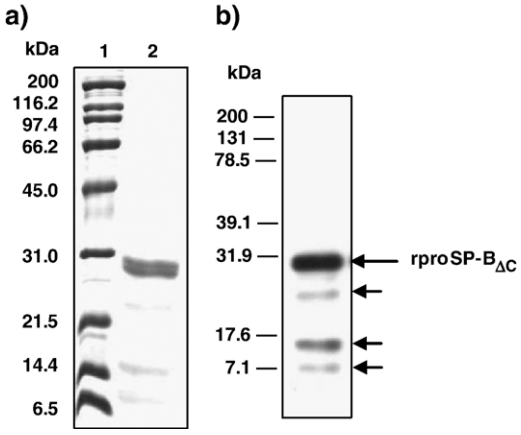

Fig. 6. SDS-PAGE and Western blot analysis of purified, refolded rproSP-$B_{\Delta C}$. (a) 12% acrylamide gel stained with Coomassie blue. Lane 1, molecular markers; lane 2, 6 μg of purified rproSP-$B_{\Delta C}$. (b) Western blot of rproSP-$B_{\Delta C}$ transferred to a nitrocellulose membrane from a 12% acrylamide gel and probed with anti-proSP-$B_{\Delta C}$ monoclonal antibody. Arrows indicate the position of rproSP-$B_{\Delta C}$ monomer (~31 kDa) and three minor peptides presumably resulting from degradation of the recombinant protein. The molecular mass of standard markers is indicated on the left of each panel.

of the other three minor components accounted for no more than 10% of the total mass of the purified protein. A final gel filtration chromatography step over Sephadex G-75 (Amersham Pharmacia Biotech) was performed to ensure complete sample homogeneity, but only a single protein peak was detected in the elution profile. All the protein mass eluted in fractions corresponding to the exclusion volume of the column, suggesting that the concentration step of protein samples required for chromatography application likely promotes protein–protein interactions, leading to the formation of aggregates. Structural characterization of rproSP-$B_{\Delta C}$ was therefore approached using the protein as obtained after refolding dialysis. Following the purification procedures described above, approximately 4 mg of highly pure rproSP-$B_{\Delta C}$ were obtained per liter of culture.

Quantitation of purified protein was initially achieved by amino acid analysis. The absorption spectrum of different quantified samples of purified protein allowed determination of the molar extinction coefficient of rproSP-$B_{\Delta C}$ at 280 nm,

$$\varepsilon^{280} = (3.47 \pm 0.15) \times 10^4 M^{-1} cm^{-1}$$

3.2. Characterization of purified recombinant rproSP-$B_{\Delta C}$

Mass spectrometry and peptide fingerprinting analysis from the SDS-PAGE band corresponding to the putative rproSP-$B_{\Delta C}$ monomer allowed identification of 10 peptides covering the major part of the amino acid sequence of the protein (Fig. 7). Almost all the predicted tryptic peptides with molecular masses falling in the analyzed *m/z* range (700–2500) were found in the peptide mass fingerprint of rproSP-$B_{\Delta C}$. Only the mass of one theoretical peptide, covering the amino acid sequence of the segment 258–269 (YSVILLDTLLGR), did not match any of the masses of the peaks in the spectrogram. On the other hand, the mass expected for the sequence 181–193 matched with

a)

THEORETICAL MASS	EXPERIMENTAL MASS	PEPTIDE	POSITION IN rproSP-$B_{\Delta C}$	KNOWN MODIFICATIONS
801.45	801.50	IQAMIPK	223-229	Q? E
1046.55	1046.62	MLPQLVCR	222-229	1xCys_PAM, 1xMSO
1110.53	1110.55	EAIFQDTMR	90-98	-
1122.60	1122.56	DPLPDPLLDK	171-180	-
1214.67	1214.57	GALAVAVAQVCR	230-241	1xCys_CAM
1238.62	1238.65	EAIFQDTMRK	90-99	-
1346.85	1346.88	LVLPVLPGALQAR*	181-193	-
1511.89	1511.79	MLPQLVCRLVLR	270-281	1xCys_PAM
1617.87	1617.88	KFLEQECNVLPLK	99-111	1xCys_PAM
2145.06	2145.06	QPEPEQEPGMSDPLPKPLR	152-170	-

b)

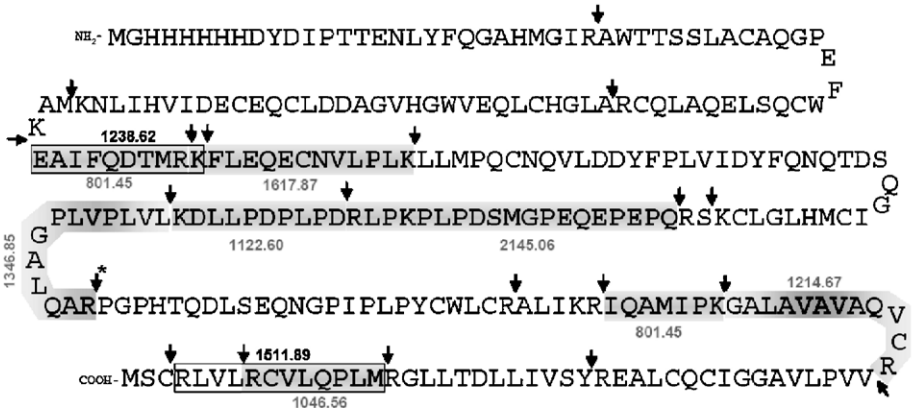

Fig. 7. Peptide mass fingerprint of rproSP-$B_{\Delta C}$. (a) The peptide mixture resulting from the in-gel digestion of rproSP-$B_{\Delta C}$ by trypsin, as described under Materials and methods, was subjected to MALDI-TOF mass spectrometry. Data were collected in the *m/z* range of 700–2500. Matched peptides are listed in the table. The theoretical mass was calculated taking into account the indicated modifications. (b) Sequence of rproSP-$B_{\Delta C}$, indicating the theoretical trypsin cleavage sites. The sequence of the identified peptides are shaded or included in a box (when overlapping). The theoretical masses taking into account the known modifications are also indicated. Q→E: glutamine hydrolysis to yield glutamic acid. Cys_CAM: cysteine reacted with iodoacetamide to yield carboxyamidomethyl cysteine. Cys_PAM: cysteine forming polyacrylamide adducts. MSO: methionine in oxidized form. * This peptide requires trypsin cleavage between RP, which is not an expected cleavage site for trypsin since this enzyme usually cleaves after basic residues not followed by proline.

precision (satisfying tolerance limits, ± 100 ppm) one of the experimental masses obtained after mass spectrometry analysis, even though the corresponding peptide would be the result of an exceptional cleavage with trypsin after an arginine residue followed by proline. As the NH_2-terminal region of rproSP-$B_{\Delta C}$ does not contain any tryptic peptide with expected molecular mass within the analyzed *m*/*z* range, the NH_2-terminal sequence of the purified protein was determined by automated Edman degradation, confirming up to 7 residues the expected N-terminal sequence: M–G–H–H–H–H–H.

Taking into account that disulfide bonds are poorly formed in the cytosol of *E. coli* and that the isolation and purification procedure used to produce rproSP-$B_{\Delta C}$ was carried out in the presence of β-mercaptoethanol, we wanted to know whether or not the protein could form disulfide bonds during or after refolding. To address this question we optimized the determination of free Cys in rproSP-$B_{\Delta C}$ by reaction with DTNB and subsequent spectrophotometric detection under native and denaturing conditions. ProSP-$B_{\Delta C}$ contains 17 cysteines, 7 within the sequence of the mature peptide and 10 in the N-terminal fragment of the recombinant protein. In the absence of denaturing agents only 11–12% of the cysteines reacted with DTNB, indicating that a major fraction of the cysteines were not accessible to the reagent under these conditions. However, in the presence of 5 M guanidinium chloride, the reaction with Ellman reagent determined that practically 80% of the cysteines remained as free Cys (–SH). Free cysteines were therefore almost completely shielded from access to the reagent in the folded protein.

The spectroscopic characterization of purified rproSP-$B_{\Delta C}$ is shown in Fig. 8. The far-UV CD spectrum shows 2 minima in ellipticity at ~210 and ~222 nm, indicative of a main α-helical secondary structure (Fig. 8a). The estimation of different secondary structure elements according to Selcon3, CDsstr and Contin programs resulted in the averaged values presented in the table of Fig. 8a. As expected, the calculated proportion of α-helix (~32%) is the main contribution to the ordered secondary structure according to the three methods of CD analysis employed.

The tertiary structure of the protein in the environment of the fluorophores was analyzed by fluorescence emission spectroscopy of the 6 tyrosines and 4 tryptophans contained in the sequence of rproSP-$B_{\Delta C}$ (Fig. 8b). Upon excitation at 275 nm the spectrum exhibited an emission maximum centred at 333 nm, shifted more than 15 nm from the position of the maximum described for free tryptophan in aqueous solution (348–350 nm) [23]. This indicates that the averaged micro-environment of the tryptophans in rproSP-$B_{\Delta C}$, probably provided by protein folding, is significantly more hydrophobic than that of a residue completely exposed to the solvent. This blue-shift of the fluorescence, together with the circular dichroism spectrum, supports the idea that the protein is properly refolded after dialysis. Moreover, emission spectra obtained upon excitation at 275 and 295 nm are practically identical, indicating an almost negligible contribution of tyrosines to the fluorescence spectrum of the protein. This contribution, lower than expected for a Trp:Tyr ratio of 4:6 is probably due to extensive resonance energy transfer from tyrosine fluorescence to nearby tryptophans and/or to quenching by other close side chains.

In order to verify that the introduction of a hydroxylamine cleavage site at the beginning of the mature SP-B sequence as well as the elimination of the endogenous hydroxylamine cleavage site in the N-terminal propeptide (see Fig. 1) did not affect the native structure of proSP-$B_{\Delta C}$, a new construct without any substitution with respect to the wild type DNA sequence of proSP-$B_{\Delta C}$ was cloned and expressed in *E. coli*. Isolation and purification of the protein was performed using the same procedure described above, and its far-UV CD and

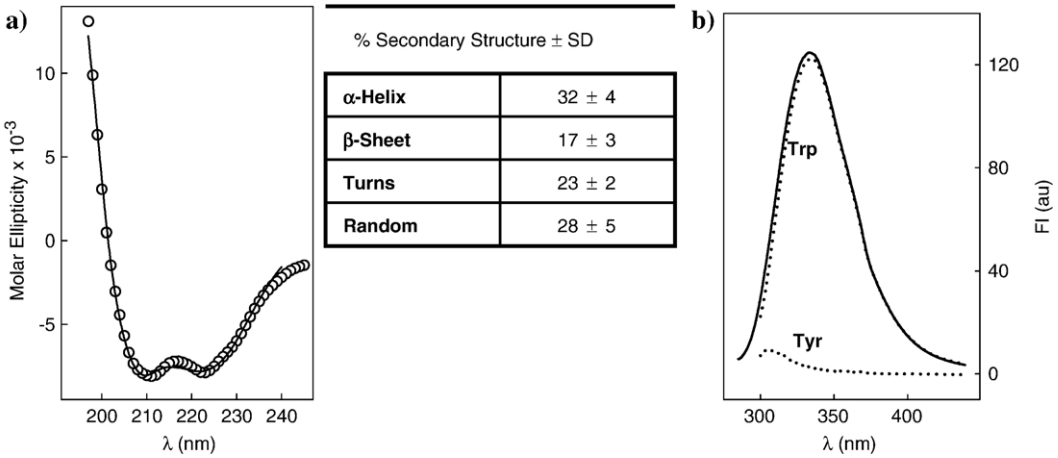

Fig. 8. Spectroscopic characterization of rproSP-$B_{\Delta C}$. (a) Far-UV circular dichroism spectrum of rproSP-$B_{\Delta C}$ in 5 mM Tris buffer pH 7 containing 150 mM of NaCl. The protein concentration was 0.1 mg/mL. The solid line represents the theoretical spectrum calculated with CONTIN program [19]. Percents of secondary structure of rproSP-$B_{\Delta C}$ were calculated from its far-UV CD spectrum using three different programs (Selcon 3, CDsstr and Contin/ll). Results are expressed in the table as means ± SD. (b) Fluorescence emission spectrum of rproSP-$B_{\Delta C}$ in the same buffer. The protein concentration was ~ 10 μg/mL and the fluorescence intensity (FI) is presented in arbitrary units (au). The solid line represents the spectrum obtained upon excitation at 275 nm. Dotted lines represent the deconvoluted contributions of tryptophans and tyrosines to the global spectrum, calculated as described under Materials and methods.

fluorescence emission spectra (not shown) were very similar to those shown in Fig. 8 (see supplementary data).

Following structural characterization, we analyzed the ability of soluble refolded rproSP-$B_{\Delta C}$ to interact with phospholipid membranes. Changes in Trp fluorescence emission of samples containing rproSP$B_{\Delta C}$ in the presence of increasing amounts of phospholipid vesicles are presented in Fig. 9. The analysis was carried out in the presence of DPPC (the major lipid component in pulmonary surfactant) as well as in the presence of unsaturated zwitterionic (POPC) or anionic (POPG) phospholipid vesicles. In all cases, a saturable increase in fluorescence intensity observed in the presence of increasing concentrations of lipid, indicates that rproSP-$B_{\Delta C}$ is able to interact with membranes of all the three phospholipid species analyzed.

The secondary structure of the protein was also studied in the presence of unilamellar vesicles of POPC or POPG by circular dichroism (CD) (Fig. 10). Both spectra exhibit CD features consistent with a mainly α-helical conformation, in similar proportions to that estimated for the protein in the absence of lipids. However, scattering problems with lipid-containing samples did not allow obtaining CD spectra with good enough signal-to-noise ratio at wavelengths lower than 200 nm, thus preventing a reliable determination of the different secondary structure proportions.

The intrinsic amphipathic structure of rproSP-$B_{\Delta C}$ is revealed by its tendency to spontaneously adsorb to an air–liquid interface. Injection of an aliquot of the protein in a surface balance is followed by an immediate increase in surface pressure (Fig. 11a), to reach surface pressures around 20 mN/m. This maximum pressure was achieved with peptide concentrations of 0.2 μM or higher. Recombinant proSP-$B_{\Delta C}$ was also

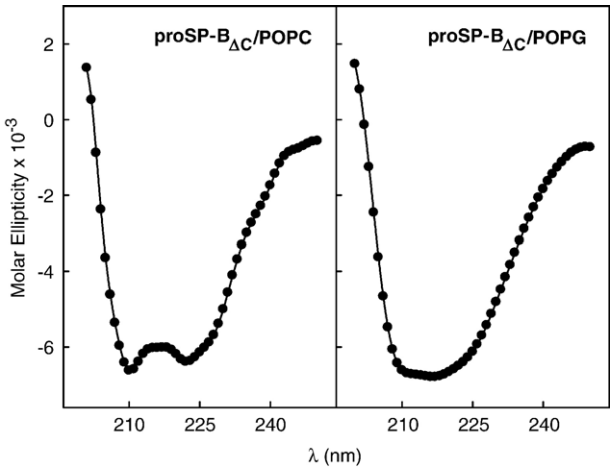

Fig. 10. Far-UV circular dichroism spectrum of rproSP-$B_{\Delta C}$ in the presence of phospholipid vesicles. The spectra were obtained in the presence of POPC or POPG unilamellar vesicles in 5 mM Tris, 5 mM Mes and 5 mM sodium acetate buffer, pH 7, containing 150 mM of NaCl. The protein concentration was 0.1 mg/mL and the protein to lipid ratio, 1:4 (by weight).

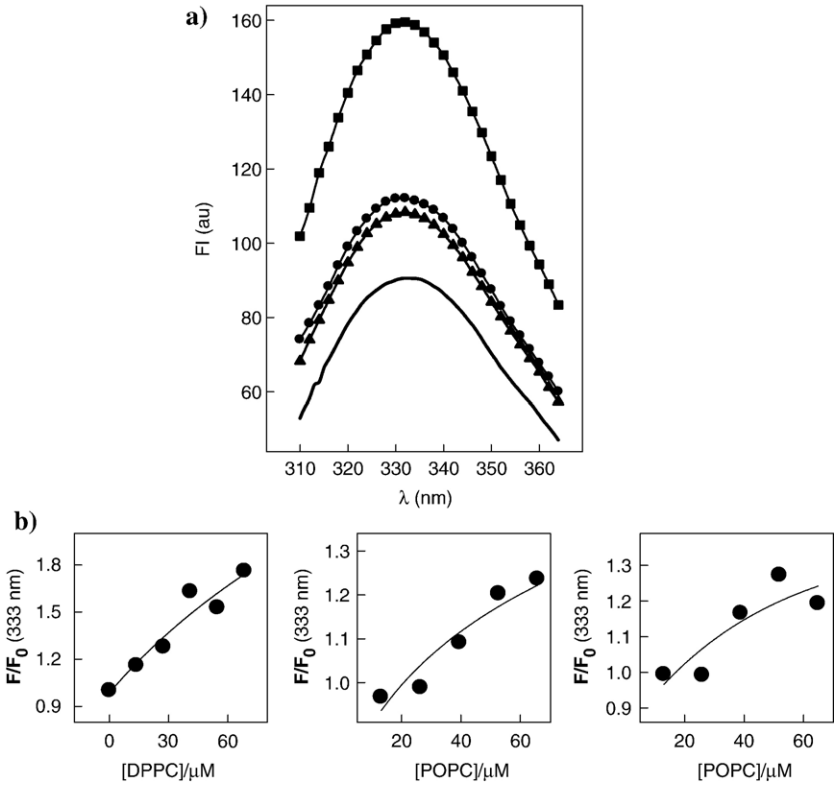

Fig. 9. Fluorescence analysis of the interaction of rproSP-$B_{\Delta C}$ with phospholipid membranes. (a) Fluorescence emission spectra of rproSP-$B_{\Delta C}$ in the absence (solid line) or in the presence of DPPC (squares), POPC (circles) or POPG (triangles) unilamellar vesicles in 5 mM Tris, 5 mM Mes and 5 mM sodium acetate buffer, pH 7, containing 150 mM of NaCl. The protein concentration was ~10 μg/mL and the lipid concentration was 50 μg/mL. (b) Dependence of the fluorescence emission intensity (FI) at 333 nm of rproSP-$B_{\Delta C}$ on the concentration of the phospholipids. F/F_0 represents the relative fluorescence intensity measured at 333 nm, where the protein exhibits the maximum FI.

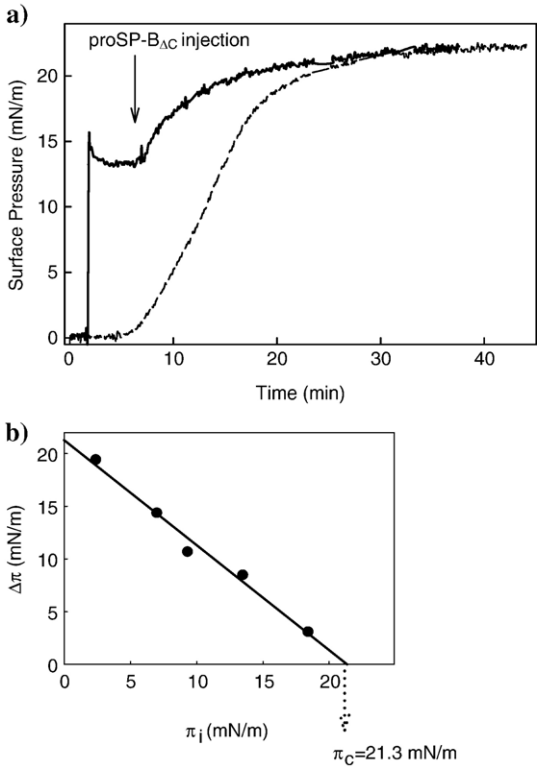

Fig. 11. Interfacial adsorption/insertion of rproSP-B$_{\Delta C}$. (a) Interfacial adsorption kinetics of rproSP-B$_{\Delta C}$ to a clean air–liquid interface (dashed line) or to a preformed DPPC:POPG, (7:3, w/w) monolayer (solid line), from a buffered subphase (5 mM Tris, pH 7, containing 150 mM NaCl). After ~5 min equilibration, 30 μL of buffer containing 11 μg of protein (0.23 μM, final concentration in the subphase) were injected into the subphase and changes in surface pressure were monitored. The experiments were run at 25 °C with continuous stirring of the subphase. (b) Increment of surface pressure ($\Delta\pi$) observed in preformed DPPC:POPG (7:3, w/w) monolayers measured 23 min after injection of rproSP-B$_{\Delta C}$ (11 μg) into the subphase, plotted vs. the initial surface pressure of the films (π_i). The critical insertion pressure (π_c) was calculated by extrapolation of the plot at $\Delta\pi$=0 mN/m.

able to associate with and perturb an interface already occupied by a DPPC:POPG (7:3, w/w) monolayer. Fig. 11a shows the insertion kinetics of the protein into a phospholipid monolayer preformed at 13.5 mN/m. Injection of rproSP-B$_{\Delta C}$ is followed by a rapid pressure increase ($\Delta\pi$) as a consequence of the association of the protein with the interfacial film. The observed $\Delta\pi$ indicated association with, and eventual insertion of the protein into the monolayer. In Fig. 11b, the increase in surface pressure ($\Delta\pi$) after injection of rproSP-B$_{\Delta C}$ has been plotted vs. the initial surface pressure (π_i) of different preexisting DPPC:POPG (7:3, w/w) monolayers. As expected, $\Delta\pi$ decreased with increasing π_i, since tighter lipid packing prevents insertion of the protein into the monolayer. From these plots one can calculate the critical insertion pressure (π_c), defined as the maximum pressure at which the protein is still able to insert. The resulting π_c for rproSP-B$_{\Delta C}$, under the experimental conditions described above, was 21.3 mN/m. This parameter depends on the monolayer composition as well as on the relative affinity of the protein to associate with the interface film. It is generally assumed that the lateral packing in a lipid bilayer can be roughly mimicked by a monolayer compressed to ~30 mN/m. Accordingly, molecules inserting against π_c values higher than 30 mN/m are usually considered competent to insert into lipid membranes [24], although the real lateral pressure and lipid packing of a free-standing membrane is a matter of discussion. A shallow membrane–protein association can still be possible when π_c values fall below this theoretical threshold of 30 mN/m, as seems to be the case for rproSP-B$_{\Delta C}$.

4. Discussion

ProSP-B, the precursor of pulmonary surfactant protein B, is a protein intermediate that cannot be isolated from natural sources in reasonable amounts to permit detailed analysis of structure and behaviour under physiologically-relevant conditions. The unprocessed precursor protein contains three well-defined domains sharing a common disulfide bond pattern that relates them to the saposin-like family of proteins (SAPLIP) [25]. The most extensively studied of these domains is the one corresponding to mature SP-B. The two flanking domains have also been identified as saposin-like domains and different authors have suggested the possibility of an independent function for each of these domains after proSP-B proteolytic processing [11,13,26,27]. One method to study proSP-B and its N- and C-terminal domains is the production of each of the domains as recombinant proteins in a heterologous system. ProSP-B (full length) and shorter forms (including a protein without the C-terminal flanking domain, SP-B$_{\Delta C}$) have been expressed in mammalian cell lines [11,12] to elucidate the structural requirements for intracellular transport and targeting of SP-B along the exocytic pathway of type II pneumocytes. More recently, these recombinant precursor forms have been expressed and purified from *E. coli* or insect cells for use as substrates to identify proteases involved in proSP-B processing in vivo [6,28]. Expression and purification of the N- and C-terminal propeptides of proSP-B have also been optimized in order to produce antibodies against these particular domains [29]. In addition, Zaltash and Johansson expressed and purified the SP-B precursor from *E. coli* to get information on the secondary structure and domain organization of the full length protein [25]. The latter is, to our knowledge, the only published work addressing some structural characterization of proSP-B.

Previous studies demonstrated that the N-terminal flanking domain and the mature peptide are sufficient to mediate appropriate targeting and processing of SP-B in type II cells in vivo [12]. Moreover, transgenic mice expressing the truncated form of proSP-B that lacked the C-terminal domain, in a null background (SP-B$^{-/-}$), survived without any evidence of respiratory problems, having normal lung function and properly processed SP-B in alveolar airspaces [13]. The goal of the present study was to express, purify and characterize the structure and lipid–protein interactions of this truncated form of the SP-B precursor (rproSP-B$_{\Delta C}$). The gene introduced was engineered to have in the future the possibility to cleave and separate afterwards the N-terminal propeptide from the mature protein.

E. coli is one of the most frequently used organisms to produce recombinant proteins because it is relatively inexpensive and

often yields high amounts of product. Although disulfide bond formation usually does not take place under reducing intracellular conditions, other SAPLIPs have been expressed in this prokaryotic system yielding active proteins after purification [30]. In addition, we have previously demonstrated that the structure, lipid–protein interactions and surface activity of an extensively reduced and alkylated form of the mature peptide (SP-Br) were all similar to the features of native SP-B purified from animal lungs. These antecedents suggest that a recombinant form of mature SP-B, even in the absence of disulfide bridges, could mimic most of the SP-B activities [22].

Recombinant proSP-$B_{\Delta C}$ has been purified from the insoluble fraction of inclusion bodies in a single chromatographic step, using a metal affinity column followed by successive dialysis to facilitate protein refolding. Direct elution of the protein from the metal affinity column in the absence of urea was previously proposed as a method to obtain folded rproSP-$B_{\Delta C}$ [31]. However, elution in urea-free buffer of the high loads of protein used in the present work produced irreversible stacking of the protein in the affinity matrix. By refolding the eluted protein through stepwise dialysis, we could produce about 4 mg of folded proSP$B_{\Delta C}$ per liter of culture. Anti-proSP-B monoclonal antibody recognition, peptide mass fingerprinting and N-terminal sequencing verified that the purified protein had the expected features of proSP-$B_{\Delta C}$.

According to the circular dichroism spectrum, purified refolded rproSP-$B_{\Delta C}$ contained a high content of ordered secondary structure including extensive α-helical structure (~32%). A similar content of α-helix (~35%) was previously estimated for proSP-B, the full length precursor of SP-B [25] also expressed in *E. coli*. The structure of the saposin-like domains has been previously addressed by CD analysis of different SAPLIPs including NK-lysin, saposins A, B, C and D, or mature SP-B. All these proteins, which contain only a single saposin-like domain, were found to be comprised of 41–53% of α-helices [32–35]. Considering that proSP-$B_{\Delta C}$ contains two saposin-like domains and a significant proportion of protein (~50%) located outside these modules, our results are compatible with the expected secondary structure of rproSP-$B_{\Delta C}$. It is remarkable that both recombinant proSP-B and recombinant proSP-$B_{\Delta C}$ were obtained as soluble proteins in aqueous buffers whereas mature SP-B has only been isolated and studied in organic solvents or lipidic environments due to its high hydrophobicity. It should be also pointed out that, according to the work of Zaltash and Johansson [25], proSP-B is stable at 8 °C for several months while our rproSP-$B_{\Delta C}$ has to be maintained at −80 °C for long term storage, suggesting that the C-terminal domain might confer stability to the recombinant protein. Zaltash and Johansson [25] reported that proSP-B behaved in their hands as a disulfide-dependent oligomer under non-reducing conditions. Recombinant proSP-$B_{\Delta C}$, as well as proSP-B expressed in type II cells and in a pulmonary adenocarcinoma cell line [36,37], was detected in the gels as a monomeric form in the absence of any reducing agent (not shown). Nevertheless, recombinant proSP-$B_{\Delta C}$ also exhibited a clear tendency to form high molecular mass oligomers that did not easily penetrate in SDS-PAGE gels. This could be at least partially driven by formation of some intermolecular disulfides. According to our results about 20% of the cysteines in rproSP-$B_{\Delta C}$ might be involved in inter- or intra-molecular disulfide bonds. Some of the intramolecular disulfides could be responsible for the apparent changes in electrophoretic mobility detected in the protein along the purification and refolding procedures, as has been shown for other proteins refolded in vitro [38,39].

On the other hand, fluorescence emission maximum of rproSP-$B_{\Delta C}$ is dominated by the contribution of tryptophan, centred at 333 nm, as expected for residues located in a hydrophobic microenvironment. These results, together with the CD data described above, suggest that refolding of rproSP-$B_{\Delta C}$ has proceeded successfully, leading to an apparently well-folded protein available for further biophysical and structural studies. The unavailability of native proSP-B isolated from natural sources makes it difficult to evaluate the extent to which rproSP-$B_{\Delta C}$ approximates a native-like conformation after refolding.

The study of the interaction of rproSP-$B_{\Delta C}$ with membranes has a notable interest related to the understanding of the mechanisms governing the trafficking, assembly and processing of SP-B precursor along the exocytic pathway of Type II pneumocytes. To our knowledge, no data had been reported so far on the membrane binding properties of the SP-B precursor. Our results indicate that water-soluble rproSP-B is able to interact with different types of phospholipid membranes, either saturated (DPPC) or unsaturated, zwiterionic (POPC) or anionic (POPG). The monolayer insertion experiments indicate, however, that rproSP-$B_{\Delta C}$ is not inserting very deep into DPPC:POPG (7:3, w/w) membranes suggesting that its lipid–protein interaction is certainly different to the deep interaction expected for mature SP-B, which is able to insert into phospholipid layers compressed up to pressures higher than 45 mN/m [40]. It is possible that the chaperon-like N-terminal propeptide maintains the whole protein in shallow association with membranes until mature SP-B is exposed and deeperly assembled into the lipids in lamellar bodies. We propose that some environmental factors such as the acidification of pH [41] or the increase in Ca2+ concentration to the values probably occurring in lamellar bodies, may be triggering factors to promote such a deeper insertion of the mature module of SP-B, which could precede or accompany the proteolytic maturation of the precursor. It is therefore conceivable that interaction of the SP-B precursor with membranes, likely in a defined orientated manner, is an important step in the assembly of the protein along its trafficking pathway. We believe that the rproSP-$B_{\Delta C}$ form produced in the present study is a useful analogue to get further insight the molecular mechanisms associated with assembly of pulmonary surfactant under physiologically-relevant conditions.

Acknowledgements

We are sincerely grateful to Prof. Timothy E. Weaver, from Cincinnati Children's Hospital, who generously provided us with several of the vectors, DNA sequences and antibodies used

in this work. We also thank Prof. Weaver for scientific advising and very fruitful discussions. The authors are also indebted to Dr. Francisco Gavilanes from the Dept. de Bioquímica y Biología Molecular I in Universidad Complutense and Dr. Javier Varela from Centro de Investigaciones Biológicas for technical assistance with amino acid analysis and N-terminal sequencing, respectively. We thank as well, Dr. Juan Pablo Albar from Centro Nacional de Biotecnología and Dra. Ma Luisa Hernáez from the Proteomics Facility of Universidad Complutense for their assistance with mass spectrometry analysis and peptide fingerprinting. Authors are also indebted to Dr. Esther Aceituno for technical assistance with the purification of some protein batches. This work has been supported by grants from the Spanish Ministry of Education and Science (BIO2003-09056 and BIO2006-03130), Community of Madrid (PMAT-000283-0505) and European Commission (CT04-007931 and CT04-5122219).

Appendix A. Supplementary data

Supplementary data associated with this article can be found, in the online version, at doi:10.1016/j.bbamem.2006.07.016.

References

[1] K.R. Melton, L.L. Nesslein, M. Ikegami, J.W. Tichelaar, J.C. Clark, J.A. Whitsett, T.E. Weaver, SP-B deficiency causes respiratory failure in adult mice, Am. J. Physiol.: Lung Cell Mol. Physiol. 285 (2003) L543–L549.

[2] L.L. Nesslein, K.R. Melton, M. Ikegami, C.L. Na, S.E. Wert, W.R. Rice, J.A. Whitsett, T.E. Weaver, Partial SP-B deficiency perturbs lung function and causes air space abnormalities, Am. J. Physiol.: Lung Cell Mol. Physiol. 288 (2005) L1154–L1161.

[3] L.M. Nogee, G. Garnier, H.C. Dietz, L. Singer, A.M. Murphy, D.E. deMello, H.R. Colten, A mutation in the surfactant protein B gene responsible for fatal neonatal respiratory disease in multiple kindreds, J. Clin. Invest. 93 (1994) 1860–1863.

[4] L.M. Nogee, S.E. Wert, S.A. Proffit, W.M. Hull, J.A. Whitsett, Allelic heterogeneity in hereditary surfactant protein B (SP-B) deficiency, Am. J. Respir. Crit. Care Med. 161 (2000) 973–981.

[5] A. Korimilli, L.W. Gonzales, S.H. Guttentag, Intracellular localization of processing events in human surfactant protein B biosynthesis, J. Biol. Chem. 275 (2000) 8672–8679.

[6] T. Ueno, S. Linder, C.L. Na, W.R. Rice, J. Johansson, T.E. Weaver, Processing of pulmonary surfactant protein B by napsin and cathepsin H, J. Biol. Chem. 279 (2004) 16178–16184.

[7] M.A. Oosterlaken-Dijksterhuis, M. van Eijk, L.M. van Golde, H.P. Haagsman, Lipid mixing is mediated by the hydrophobic surfactant protein SP-B but not by SP-C, Biochim. Biophys. Acta 1110 (1992) 45–50.

[8] F.R. Poulain, L. Allen, M.C. Williams, R.L. Hamilton, S. Hawgood, Effects of surfactant apolipoproteins on liposome structure: implications for tubular myelin formation, Am. J. Physiol. 262 (1992) L730–L739.

[9] F.R. Poulain, S. Nir, S. Hawgood, Kinetics of phospholipid membrane fusion induced by surfactant apoproteins A and B, Biochim. Biophys. Acta 1278 (1996) 169–175.

[10] M.A. Ryan, X. Qi, A.G. Serrano, M. Ikegami, J. Perez-Gil, J. Johansson, T.E. Weaver, Mapping and analysis of the lytic and fusogenic domains of surfactant protein B, Biochemistry 44 (2005) 861–872.

[11] S. Lin, K.S. Phillips, M.R. Wilder, T.E. Weaver, Structural requirements for intracellular transport of pulmonary surfactant protein B (SP-B), Biochim. Biophys. Acta 1312 (1996) 177–185.

[12] S. Lin, H.T. Akinbi, J.S. Breslin, T.E. Weaver, Structural requirements for targeting of surfactant protein B (SP-B) to secretory granules in vitro and in vivo, J. Biol. Chem. 271 (1996) 19689–19695.

[13] H.T. Akinbi, J.S. Breslin, M. Ikegami, H.S. Iwamoto, J.C. Clark, J.A. Whitsett, A.H. Jobe, T.E. Weaver, Rescue of SP-B knockout mice with a truncated SP-B proprotein. Function of the C-terminal propeptide, J. Biol. Chem. 272 (1997) 9640–9647.

[14] D. Polayes, J. Hughes, Efficient protein expression and simple purification using the pProEx-1 system, Focus 16 (1994) 81–84.

[15] S. Sechi, B.T. Chait, Modification of cysteine residues by alkylation. A tool in peptide mapping and protein identification, Anal. Chem. 70 (1998) 5150–5158.

[16] G.L. Ellman, A colorimetric method for determining low concentrations of mercaptans, Arch. Biochem. Biophys. 74 (1958) 443–450.

[17] G.L. Ellman, Tissue sulfhydryl groups, Arch. Biochem. Biophys. 82 (1959) 70–77.

[18] M.L. Ruano, I. Garcia-Verdugo, E. Miguel, J. Perez-Gil, C. Casals, Self-aggregation of surfactant protein A, Biochemistry 39 (2000) 6529–6537.

[19] N. Sreerama, R.W. Woody, Estimation of protein secondary structure from circular dichroism spectra: comparison of CONTIN, SELCON, and CDSSTR methods with an expanded reference set, Anal. Biochem. 287 (2000) 252–260.

[20] N. Sreerama, R.W. Woody, On the analysis of membrane protein circular dichroism spectra, Protein Sci. 13 (2004) 100–112.

[21] E. Nuñez, X. Wei, C. Delgado, I. Rodriguez-Crespo, B. Yelamos, J. Gomez-Gutierrez, D.L. Peterson, F. Gavilanes, Cloning, expression, and purification of histidine-tagged preS domains of hepatitis B virus, Protein Expr. Purif. 21 (2001) 183–191.

[22] A.G. Serrano, A. Cruz, K. Rodriguez-Capote, F. Possmayer, J. Perez-Gil, Intrinsic structural and functional determinants within the amino acid sequence of mature pulmonary surfactant protein SP-B, Biochemistry 44 (2005) 417–430.

[23] J.R. Lakowicz, Principles of Fluorescence Spectroscopy, Plenum Press, New York, 1999.

[24] H. Brockman, Lipid monolayers: why use half a membrane to characterize protein–membrane interactions? Curr. Opin. Struct. Biol. 9 (1999) 438–443.

[25] S. Zaltash, J. Johansson, Secondary structure and limited proteolysis give experimental evidence that the precursor of pulmonary surfactant protein B contains three saposin-like domains, FEBS Lett. 423 (1998) 1–4.

[26] H.T. Akinbi, P. Markart, R. Epaud, Z.C. Chroneos, T.E. Weaver, Antibacterial properties of surfactant protein B in innate host defense of the lung, (2005).

[27] S. Hawgood, Surfactant protein B: structure and function, Biol. Neonate 85 (2004) 285–289.

[28] F. Brasch, M. Ochs, T. Kahne, S. Guttentag, V. Schauer-Vukasinovic, M. Derrick, G. Johnen, N. Kapp, K.M. Muller, J. Richter, T. Giller, S. Hawgood, F. Buhling, Involvement of napsin A in the C- and N-terminal processing of surfactant protein B in type-II pneumocytes of the human lung, J. Biol. Chem. 278 (2003) 49006–49014.

[29] F. Brasch, G. Johnen, A. Winn-Brasch, S.H. Guttentag, A. Schmiedl, N. Kapp, Y. Suzuki, K.M. Muller, J. Richter, S. Hawgood, M. Ochs, Surfactant protein B in type II pneumocytes and intra-alveolar surfactant forms of human lungs, Am. J. Respir. Cell Mol. Biol. 30 (2004) 449–558.

[30] X. Qi, T. Leonova, G.A. Grabowski, Functional human saposins expressed in *Escherichia coli*. Evidence for binding and activation properties of saposins C with acid beta-glucosidase, J. Biol. Chem. 269 (1994) 16746–16753.

[31] A. Holzinger, K.S. Phillips, T.E. Weaver, Single-step purification/solubilization of recombinant proteins: application to surfactant protein B, BioTechniques 20 (1996) 804–806 (808).

[32] M. Andersson, T. Curstedt, H. Jornvall, J. Johansson, An amphipathic helical motif common to tumourolytic polypeptide NK-lysin and pulmonary surfactant polypeptide SP-B, FEBS Lett. 362 (1995) 328–332.

[33] J.S. O'Brien, Y. Kishimoto, Saposin proteins: structure, function, and role in human lysosomal storage disorders, FASEB J. 5 (1991) 301–308.

[34] J. Perez-Gil, A. Cruz, C. Casals, Solubility of hydrophobic surfactant proteins in organic solvent/water mixtures. Structural studies on SP-B and

SP-C in aqueous organic solvents and lipids, Biochim. Biophys. Acta 1168 (1993) 261–270.
[35] A.J. Waring, Y. Chen, K.F. Faull, R. Stevens, M.A. Sherman, A.L. Fluharty, Porcine cerebroside sulfate activator (saposin B) secondary structure: CD, FTIR, and NMR studies, Mol. Genet. Metab. 63 (1998) 14–25.
[36] S. Hawgood, D. Latham, J. Borchelt, D. Damm, T. White, B. Benson, J.R. Wright, Cell-specific posttranslational processing of the surfactant-associated protein SP-B, Am. J. Physiol. 264 (1993) L290–L299.
[37] M.A. O'Reilly, T.E. Weaver, T.J. Pilot-Matias, V.K. Sarin, A.F. Gazdar, J.A. Whitsett, In vitro translation, post-translational processing and secretion of pulmonary surfactant protein B precursors, Biochim. Biophys. Acta 1011 (1989) 140–148.
[38] M.A. Kaderbhai, B.M. Austen, Studies on the formation of intrachain disulphide bonds in newly biosynthesised bovine prolactin. Role of protein-disulphide isomerase, Eur. J. Biochem. 153 (1985) 167–178.
[39] H. Lee, H.K. Kim, J.H. Lee, W.K. You, S.I. Chung, S.I. Chang, M.H. Park, Y.K. Hong, Y.A. Joe, Disruption of interkringle disulfide bond of plasminogen kringle 1–3 changes the lysine binding capability of kringle 2, but not its antiangiogenic activity, Arch. Biochem. Biophys. 375 (2000) 359–363.
[40] A. Cruz, L.A. Worthman, A.G. Serrano, C. Casals, K.M. Keough, J. Perez-Gil, Microstructure and dynamic surface properties of surfactant protein SP-B/dipalmitoylphosphatidylcholine interfacial films spread from lipid–protein bilayers, Eur. Biophys. J. 29 (2000) 204–213.
[41] M.F. Beers, Inhibition of cellular processing of surfactant protein C by drugs affecting intracellular pH gradients, J. Biol. Chem. 271 (1996) 14361–14370.